

Photochemical Oxidation of Pt(IV)Me₃(1,2-diimine) Thiolates to Luminescent Pt(IV) Sulfinates

Barbora Mala,^{||} Laura E. Murtagh,^{||} Charlotte M. A. Farrow, Geoffrey R. Akien, Nathan R. Halcovich, Sarah L. Allinson, James A. Platts, and Michael P. Coogan*



Cite This: <https://doi.org/10.1021/acs.inorgchem.0c03553>



Read Online

ACCESS |



Metrics & More

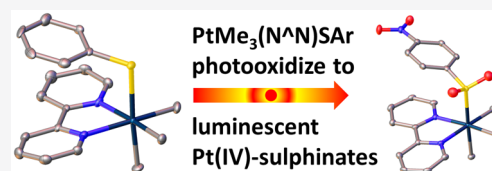


Article Recommendations



Supporting Information

ABSTRACT: We report the formation of dinuclear complexes from, and photochemical oxidation of, (CH₃)₃Pt(IV)(N[^]N) (N[^]N = 1,2-diimine derivatives) complexes of thiophenolate ligands to the analogous sulfinates (CH₃)₃Pt(N[^]N)(SO₂Ph) and structural, spectroscopic, and theoretical studies of the latter revealing tunable photophysics depending upon the 1,2-diimine ligands. Electron-rich thiolate and conjugated 1,2-diimines encourage formation of thiolate-bridged dinuclear complexes; smaller 1,2-diimines or electron-poor thiolates favor mononuclear complexes. Photooxidation of the thiolate ligand yields hitherto unreported Pt(IV)-SO₂R complexes, promoted by electron-deficient thiolates such as 4-nitrothiophenol, which exclusively forms the sulfinato complex. Such complexes exhibit expected absorptions due to π - π^* ligand transitions of the 1,2-diimines mixed with spin-allowed singlet MLCT (d - π^*) at relatively high energy (270–290 nm), as well as unexpected broad, lower energy absorptions between 360 and 490 nm. DFT data indicate that these low energy absorption bands result from excitation of Pt–S and Pt–C σ -bonding electrons to π^* orbitals on sulfinato and 1,2-diimine, the latter of which gives rise to emission in the visible range.



INTRODUCTION

There are many applications of photophysically active transition-metal complexes in, among other areas, photocatalysis,¹ LEDs and related devices,² energy-related research and photovoltaics,³ and luminescent cell imaging.⁴ There are many well-known luminescent platinum-based systems, most involving d^8 Pt(II) complexes, in particular tridentate cyclometallates derived from aromatic heterocycles with high quantum yields⁵ and impressive 2-photon cross sections.⁶ Certain platinum(IV) complexes also have useful photophysical properties including photoluminescence, with some showing quantum yields up to 80%.⁷ Luminescent bis-cyclometalated Pt(IV) complexes, of the general formula [Pt(C[^]N)₂(R)Cl], were first reported in 1984 by Chassot et al.,⁸ and since then more brightly luminescent platinum(IV) complexes with high quantum yields and long luminescence lifetimes have been reported.⁷ Cyclometalated Pt(IV) complexes are of particular interest as their properties, such as solubility and lipophilicity, are easily tunable by only slight alterations of the ligands.⁹ Furthermore, some luminescent tris-cyclometalated Pt(IV) complexes have displayed promising intense emission which is also highly sensitive to quenching by oxygen, making these potentially useful for oxygen sensing applications.¹⁰ Pt(IV)Me₃I, the first transition-metal σ -alkyl complex ever reported,¹¹ is commercially available and exists as an iodide-bridged tetramer and readily reacts with chelating N[^]N ligands to give mononuclear complexes of the general formula PtMe₃(N[^]N)X, analogous to the well-known luminophores Re(CO)₃(N[^]N)(X) (X = Cl/Br) which have

been widely applied in sensing and imaging. The photochemistry and photophysics of the Pt(IV)(N[^]N) core have been widely studied,¹² and there are several reports of thiolato derivatives of this unit.¹³

There is one report exploring the synthesis, photophysics, and application in fluorescent cell imaging, of platinum(IV) 1,2-diimine trimethyl thiolates.¹⁴ Time-dependent density functional theory calculations revealed that the excited states of platinum(IV) trimethyl 1,2-diimine iodide complexes arise from a mixed n and σ - π^* Inter-Ligand Charge Transfer (ILCT) from the lone pair of sulfur and the S–Pt σ -bond, to the 1,2-diimine π^* .¹⁴ The small range of 1,2-diimines reported indicated that absorption and emission were tunable by variations in ligand substitution, with emission extending into the NIR in one case. Therefore, in an effort to develop analogues with a variety of useful photophysical properties, an investigation of complexes based on this general structure with a range of 1,2-diimine and thiolate ligands was undertaken.

EXPERIMENTAL SECTION

General Experimental. The starting materials, reagents, and solvents used are all commercially available. ¹H NMR and ¹³C NMR

Received: December 4, 2020

spectra were recorded at 400 and 100 MHz, respectively, on a Bruker Avance III 400 and referenced to residual solvent peaks. Chemical shifts are reported in ppm, and coupling constants in Hz. All photophysical measurements were recorded in acetonitrile at 20 °C. UV–vis spectra were recorded on an Agilent Technologies Cary 60. IR spectra were recorded on an Agilent Technologies Cary 630 FTIR Spectrometer as solids and are reported in wavenumbers (cm^{-1}). Mass spectra were recorded on a Shimadzu LCMS-IT-TOF in ESI+ mode.

Steady state emission and excitation spectra were recorded on an Agilent Technologies Cary Eclipse. Luminescence lifetimes were recorded on a PicoQuant FluoTime 300 exciting with an LDH-P-C-375 or LDH-P-C405 ps pulsed laser (PicoQuant) operating at 50 and 80 MHz, respectively. The emission signals were digitized using a high-resolution TCSPC module (PicoHarp 300, PicoQuant) with 25 ps time width per channel. The time-resolved decay curves were analyzed using FLUOFIT software (PicoQuant) using a one-exponential model. Quantum yields were estimated relative to $[\text{Ru}(\text{bpy})_3] \cdot 2\text{PF}_6$ in aerated acetonitrile with titration to equi-absorbing solutions at the excitation wavelengths at around $\lambda = 0.05$. Degassed measurements were recorded in a quartz cuvette fused to a T-piece connecting a round-bottom flask and a J. Young tap connecting a ground glass joint, following three cycles of freeze-pump-thaw degassing. Iodotrimethyl($\text{N}^{\wedge}\text{N}$)Pt(IV) complexes **1–5** ($\text{N}^{\wedge}\text{N} = 2,2'$ -bipyridine (bpy) **1**, 4,4'-dimethoxy-2,2'-bipyridine (OMebpy) **2**, 1,10-phenanthroline (phen) **3**, 4,7-diphenyl-1,10-phenanthroline (Bphen) **4**, dipyrro[3,2-*a*:2',3'-*c*]phenazine (DPPZ) **5**) were prepared by literature procedures.^{12,14} Complexes **6–25** derived from the reactions of **1–5** with thiophenol, and derivatives, were metastable, and for details relating to their detection, partial characterization by crystallography and in some cases NMR and for details of the mechanistic studies and the preparation of an authentic sample of 4-mercaptomethylbenzoate disulfide,¹⁵ see the [Supporting Information \(SI\)](#).

[PtMe₃(bpy)SO₂PhNO₂] 26. To a flask containing $[\text{PtMe}_3\text{I}(2,2'$ -bipyridine)] **1** (101.3 mg, 0.19 mmol), 4-nitrothiophenol (30.0 mg, 0.19 mmol), and NaO^tBu (20.6 mg, 0.21 mmol) were added acetonitrile (4 mL) and water (1 mL), and the mixture was heated at 60 °C for 30 min, then cooled to room temperature, and refrigerated overnight, giving a solution containing orange crystals and a white powder. The mixture was filtered and washed with water to obtain orange crystals **26** (63.1 mg, 57%).

$\delta^1\text{H}$ NMR (400 MHz, CD_3CN): 8.79 (2H, d, $J = 6.5$ Hz, H6/6'; ^{195}Pt satellite $J = 19.5$ Hz), 8.19 (2H, d, $J = 8.2$ Hz, H3/3'), 8.07 (2H, t, $J = 7.9$ Hz, H4/4'), 7.67 (2H, t, $J = 6.6$, H5/5'), 7.34 (2H, d, $J = 8.9$ Hz, H8/8'), 6.58 (2H, d, $J = 9.1$ Hz, H7/7'), 1.17 (6H, s, eq-Me; ^{195}Pt satellite $J = 70.2$ Hz), 0.32 (3H, s, ax-Me; ^{195}Pt satellite $J = 66.2$ Hz); ^{13}C NMR 158.8, 154.1, 146.6 (^{195}Pt satellite $J = 14.3$ Hz) 139.0, 134.2 (^{195}Pt satellite $J = 6.3$ Hz), 127.1 (^{195}Pt satellite $J = 14.4$ Hz), 123.9 (^{195}Pt satellite $J = 8.5$ Hz), 121.5, -0.8 (^{195}Pt satellites obscured by solvent signal), -6.4 (^{195}Pt satellite $J = 677.1$ Hz); IR ν_{max} (cm^{-1}) 2892, 2812, 1559, 1491, 1418, 1219; Crystal data for **26** $\text{C}_{19}\text{H}_{21}\text{N}_3\text{O}_4\text{PtS}$ ($M = 582.54$ g/mol): triclinic, space group $P\bar{1}$ (no. 2), $a = 6.96733(19)$ Å, $b = 8.8748(2)$ Å, $c = 15.4326(4)$ Å, $\alpha = 93.374(2)^\circ$, $\beta = 92.851(2)^\circ$, $\gamma = 92.314(2)^\circ$, $V = 950.52(4)$ Å³, $Z = 2$, $T = 100.00(10)$ K, $\mu(\text{Mo K}\alpha) = 7.523$ mm⁻¹, $D_{\text{calc}} = 2.035$ g/cm³, 21 289 reflections measured ($6.802^\circ \leq 2\theta \leq 59.066^\circ$), 4782 unique ($R_{\text{int}} = 0.0372$, $R_{\text{sigma}} = 0.0267$) which were used in all calculations. The final R_1 was 0.0181 ($I > 2\sigma(I)$) and wR_2 was 0.0410 (all data). CCDC 2013232.

[PtMe₃(1,10-phenanthroline)SO₂PhNO₂] 27. To a flask containing $[\text{PtMe}_3\text{I}(1,10\text{-phenanthroline})]$ **3** (24.9 mg, 0.05 mmol), 4-nitrothiophenol (7.40 mg, 0.05 mmol), and NaO^tBu (5.2 mg, 0.05 mmol) were added acetonitrile (4 mL) and water (1 mL), and the mixture was heated at 60 °C for 30 min, then cooled to room temperature, and refrigerated overnight, giving a solution containing orange crystals and a white powder. The mixture was filtered and washed with water to obtain orange crystals **27** (19.6 mg, 71%).

$\delta^1\text{H}$ NMR (400 MHz, CDCl_3): 9.14 (2H, d, $J = 5.0$ Hz, H2/2'; ^{195}Pt satellite $J = 19.1$), 8.59 (2H, d, $J = 8.3$ Hz, H4/4'), 8.03–7.98

(4H, m, H5/5' and H3/3'), 6.92 (2H, d, $J = 8.9$ Hz, H7/7'), 6.16 (2H, d, H6/6'), 1.33 (6H, s, eq-Me; ^{195}Pt satellite $J = 70.9$ Hz), 0.40 (3H, s, ax-Me; ^{195}Pt satellite $J = 66.4$ Hz); $\delta^{13}\text{C}$ NMR (400 MHz, CDCl_3) 157.4, 146.5 (^{195}Pt satellite $J = 15.2$ Hz), 145.5, 142.8, 137.2, 133.7 (^{195}Pt satellite $J = 5.2$ Hz), 130.8 (^{195}Pt satellite $J = 6.4$ Hz), 127.4, 125.3 (^{195}Pt satellite $J = 14.0$ Hz), 120.8, -0.0 , -5.7 (^{195}Pt satellite $J = 681.8$ Hz); IR ν_{max} (cm^{-1}) 2886, 2808, 1567, 1483, 1425, 1219; Crystal data for **27** $\text{C}_{21}\text{H}_{21}\text{N}_3\text{O}_4\text{PtS}$ ($M = 606.56$ g/mol): monoclinic, space group $P2_1/n$ (no. 14), $a = 6.87831(12)$ Å, $b = 13.65275(18)$ Å, $c = 21.0623(3)$ Å, $\beta = 97.2931(15)^\circ$, $V = 1961.91(5)$ Å³, $Z = 4$, $T = 99.99(10)$ K, $\mu(\text{Cu K}\alpha) = 14.681$ mm⁻¹, $D_{\text{calc}} = 2.054$ g/cm³, 19 671 reflections measured ($7.736^\circ \leq 2\theta \leq 152.948^\circ$), 4087 unique ($R_{\text{int}} = 0.0423$, $R_{\text{sigma}} = 0.0255$) which were used in all calculations. The final R_1 was 0.0365 ($I > 2\sigma(I)$) and wR_2 was 0.0967 (all data). CCDC 2013233.

[PtMe₃(4,7'-diphenyl-1,10-phenanthroline)SO₂PhNO₂] 28. To a flask containing $[\text{PtMe}_3\text{I}(4,7'\text{-diphenyl-1,10-phenanthroline})]$ **4** (25.7 mg, 0.04 mmol), 4-nitrothiophenol (5.9 mg, 0.04 mmol), and NaO^tBu (3.9 mg, 0.04 mmol) were added acetonitrile (4 mL) and water (1 mL), and the mixture was heated at 60 °C for 30 min, then cooled to room temperature, and refrigerated overnight, giving a solution containing orange crystals and a white powder. The mixture was filtered and washed with water to obtain orange crystals **28** (10.3 mg, 38%).

$\delta^1\text{H}$ NMR (400 MHz, CDCl_3): 9.18 (2H, d, $J = 5.2$ Hz, H2/2'; ^{195}Pt satellite $J = 19.3$), 7.91 (2H, s, H4/4'), 7.85 (2H, d, 5.2 Hz, H3/3'), 7.67–7.51 (10H, m, Ph), 7.11 (2H, 9.0 Hz, d, H9/9'), 6.44 (2H, 6.4 Hz, d, H8/8'), 1.45 (6H, s, eq-Me; ^{195}Pt satellite $J = 70.0$ Hz), 0.53 (3H, s, ax-Me; ^{195}Pt satellite $J = 66.6$ Hz); $\delta^{13}\text{C}$ NMR (400 MHz, CDCl_3) 156.9, 150.5, 146.0, 145.8 (^{195}Pt satellite $J = 14.7$ Hz), 143.0, 135.6, 134.0, 129.8, 129.5, 129.2, 129.1, 125.6, 125.4, 120.8, 0.1, -5.4 (^{195}Pt satellite $J = 678.0$ Hz); IR ν_{max} (cm^{-1}) 2890, 2812, 1560, 1489, 1217; Crystal data for **28** $\text{C}_{33}\text{H}_{29}\text{N}_3\text{O}_4\text{PtS}$ ($M = 758.74$ g/mol): monoclinic, space group $C2/c$ (no. 15), $a = 21.3317(3)$ Å, $b = 12.75780(10)$ Å, $c = 24.8460(3)$ Å, $\beta = 110.718(2)^\circ$, $V = 6324.47(15)$ Å³, $Z = 8$, $T = 100.0(3)$ K, $\mu(\text{Cu K}\alpha) = 9.245$ mm⁻¹, $D_{\text{calc}} = 1.594$ g/cm³, 48 486 reflections measured ($7.608^\circ \leq 2\theta \leq 152.926^\circ$), 6617 unique ($R_{\text{int}} = 0.0305$, $R_{\text{sigma}} = 0.0135$) which were used in all calculations. The final R_1 was 0.0437 ($I > 2\sigma(I)$) and wR_2 was 0.0987 (all data). CCDC 2013234.

[PtMe₃(dipyrido[3,2-*a*:2',3'-*c*]phenazine)SO₂PhNO₂] 29. To a flask containing $[\text{PtMe}_3\text{I}(\text{dipyrido}[3,2-*a*:2',3'-*c*]phenazine)]$ **5** (25.5 mg, 0.04 mmol), 4-nitrothiophenol (6.2 mg, 0.04 mmol), and NaO^tBu (4.5 mg, 0.04 mmol) were added acetonitrile (4 mL) and water (1 mL), and the mixture was heated at 60 °C for 30 min, then cooled to room temperature, and refrigerated overnight, giving a solution containing orange crystals and a white powder. The mixture was filtered and washed with water to obtain orange crystals **29** (20.1 mg, 76%).

$\delta^1\text{H}$ NMR (400 MHz, CDCl_3): 9.80 (2H, d, $J = 8.2$ Hz, H4/4'), 9.18 (2H, d, $J = 5.1$ Hz, H2/2'; ^{195}Pt satellite $J = 18.7$), 8.50–8.44 (2H, m, H5/5'), 8.10–8.05 (4H, m, H6/6' and H3/3'), 7.02 (2H, d, $J = 8.9$, H8/8'), 6.48 (2H, d, $J = 8.9$, H7/7'), 1.44 (6H, s, eq-Me; ^{195}Pt satellite $J = 70.5$ Hz), 0.53 (3H, s, ax-Me; ^{195}Pt satellite $J = 64.6$ Hz); **29** was insufficiently soluble to collect ^{13}C data. IR ν_{max} (cm^{-1}) 2892, 2812, 1560, 1491, 1418, 1221; Crystal data for **29** $\text{C}_{27}\text{H}_{23}\text{N}_5\text{O}_4\text{PtS}$ ($M = 708.65$ g/mol): monoclinic, space group $P2_1/m$ (no. 11), $a = 7.98930(10)$ Å, $b = 13.0769(2)$ Å, $c = 12.1911(2)$ Å, $\beta = 97.1620(10)^\circ$, $V = 1263.73(3)$ Å³, $Z = 2$, $T = 215.00(10)$ K, $\mu(\text{Cu K}\alpha) = 11.536$ mm⁻¹, $D_{\text{calc}} = 1.862$ g/cm³, 13 560 reflections measured ($7.308^\circ \leq 2\theta \leq 153.144^\circ$), 2755 unique ($R_{\text{int}} = 0.0501$, $R_{\text{sigma}} = 0.0320$) which were used in all calculations. The final R_1 was 0.0496 ($I > 2\sigma(I)$) and wR_2 was 0.1303 (all data). CCDC 2013235.

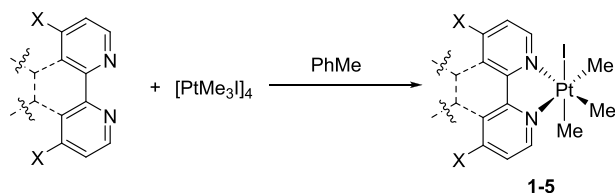
Computational Procedures. DFT calculations used Gaussian09:¹⁶ geometry optimization of **26** was performed using M06-2X/6-31+G(d,p) with SDD ECP/basis on Pt,¹⁷ which retains the stacking interaction between bpy and Ar-NO₂. Predicted absorption spectra and orbital plots were obtained from CAM-B3LYP¹⁸ with the same basis set as optimization, in PCM simulation of CH₃CN.¹⁹

Crystal structures were solved and refined using OLEX²⁰ running the SHELX²¹ suite of programs and images generated in ORTEP.²²

RESULTS AND DISCUSSION

Reactions of Iodotrimethyl Platinum(IV) 1,2-Diimines with Thiophenolates. Following the literature precedent,^{12,14} iodotrimethylplatinum(IV) 1,2-diimines were prepared from reaction of [PtMe₃I]₄ with the relevant 1,2-diimine ligand (i.e., N[^]N = 2,2'-bipyridine (bpy) **1**, 4,4'-dimethoxy-2,2'-bipyridine (OMebpy) **2**, 1,10-phenanthroline (phen) **3**, 4,7-diphenyl-1,10-phenanthroline (Bphen) **4**, dipyrdo[3,2-*a*:2',3'-*c*]phenazine (DPPZ) **5**) in toluene at reflux in good to excellent yields (Scheme 1). The DPPZ derivative **5** had low

Scheme 1. Synthesis of Iodotrimethylplatinum(IV) Complexes 1–5^a

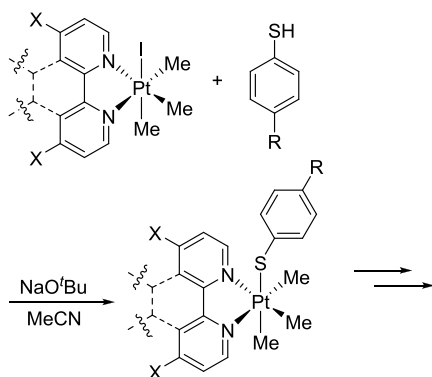


^a**1** = Bpy, **2** = di-OMebpy, **3** = phen, **4** = Bphen, **5** = DPPZ.

solubility in all solvents; however, despite the small size of the crystals obtained, X-ray data of sufficient quality to establish connectivity were obtained, confirming the identity of the product.

Attempts to prepare the thiolate complexes derived from iodoplatinum species **1–5** following literature precedent (Scheme 2),¹⁴ however, led not to the expected products but

Scheme 2. General Reaction of Iodotrimethylplatinum(IV) 1,2-Diimines with Thiophenols^a



^aR, X = H, CO₂Me, OMe, NO₂.

to a series of metastable complexes which were not fully characterized, but the identity of some were established by NMR and X-ray crystallography. NMR (see SI) indicated that an equilibrium existed between mononuclear and dinuclear products in many cases, e.g., **6** and **7** from the reaction of **5** with 4-mercaptomethylbenzoate (Scheme 3, Figure 1), and examples of the dinuclear structures were also confirmed by X-ray crystallography.

In other cases, NMR analysis indicated the presence of only mononuclear species, and X-ray crystallography showed either the expected mononuclear thiophenolate complex or a

sulfinate complex in which the coordinated sulfur had acquired two oxygen atoms. Examples of these are given in Scheme 4 and Figure 2 (thiolate **11**) and Scheme 5 and Figure 3 (sulfinate **12**), and the rest of the observed species are summarized in Table 1. Further details are available in the SI. Again, attempts to purify and characterize these species, with the exception of those derived from 4-nitrothiophenol, led to decomposition to complex product mixtures.

Regardless of the unstable nature of the products, crystallographic characterization of these species was interesting as an addition to the previously known S-bridged multinuclear Pt(IV)Me₃ species,²³ and revealing the first examples of crystallographically characterized Pt(IV) sulfinate complexes.

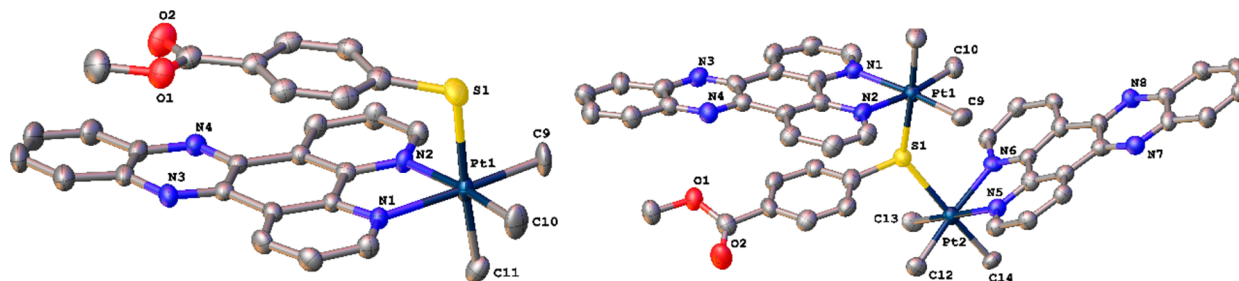
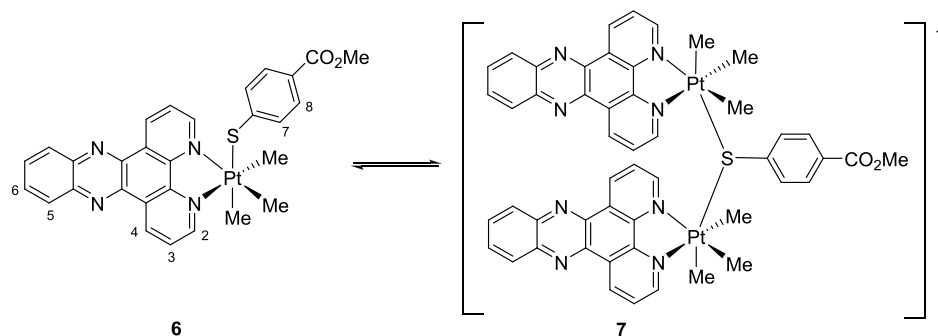
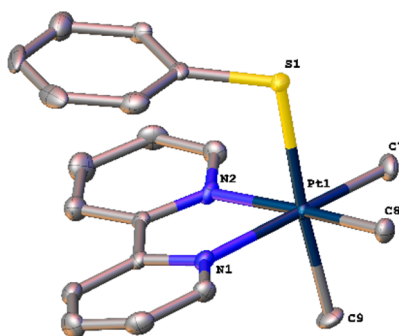
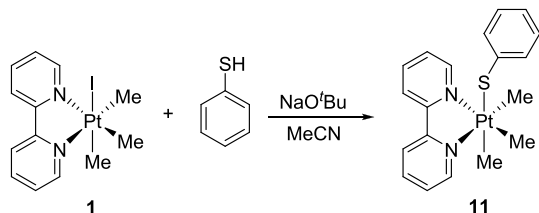
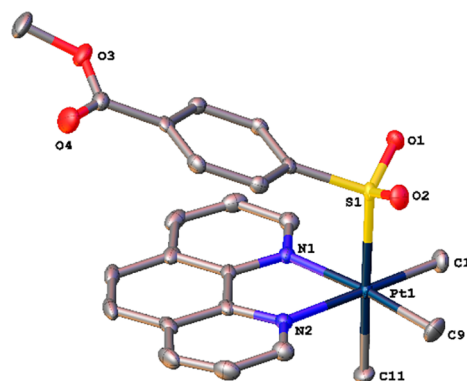
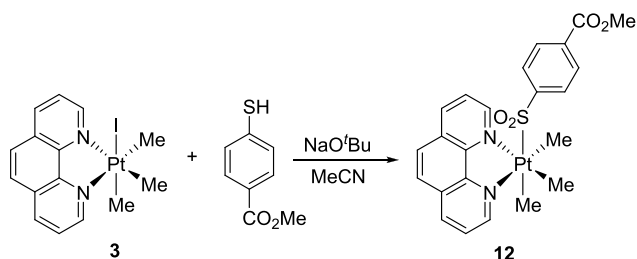
Although many of these complexes are metastable and not fully characterized, the observations of cases in which dinuclear complexes (**7**, **9**, **14**, **16**) were apparent in the NMR spectra suggest that electron-rich thiolate and conjugated 1,2-diimines encourage formation of thiolate-bridged dinuclear complexes, whereas the cases in which mononuclear species dominate (**11**, **13**, **15**, **21**, **30**) suggest that smaller 1,2-diimines or electron-poor thiolates favor mononuclear complexes.

Structural Studies of Thiolate and Sulfinate Complexes of the PtMe₃(N[^]N) Core. X-ray crystallography showed that all products form distorted octahedra whether in mononuclear or dinuclear form. Table 2 summarizes the bond lengths of most interest. The Pt–S bonds are all of similar lengths; however, the Pt–S bonds in sulfinate complexes (**12**, **17**, **26–29**) are shorter than those in the other complexes. A search of the Cambridge Crystallographic Data Centre for structures containing the Pt–SO₂R unit found only 23 reports of this substructure, of these 20 were cyclic^{24–27} (i.e., contained a chelating O₂S[^]D unit, D = donor atom), meaning that only three unsupported Pt–SO₂ bonds have previously been characterized, and there were no Pt(IV) sulfates reported.

Even though the number of crystal structures containing Pt–SO₂R bonds is limited, a few of the reports highlight Pt–S bond shortening upon oxidation of sulfur.^{25,26} This is unexpected as one would expect this bond to get longer as the sulfur becomes a weaker sigma donor. However, there are reported to be three factors that determine the M–S bond length, from analogy with Ni–S complexes. In these too, shortening of the Ni–S bond was also observed with increasing sulfur oxidation.²⁸ Although the sulfur becomes a poorer sigma donor as it is oxidized, the sulfur atom also contracts in size upon oxidation, and there is less electronic repulsion between the metal *d*-orbitals and sulfur due to loss of its lone pairs. Overall, the latter two effects dominate over the reduced sigma donation, thus resulting in a shorter Pt–S bond length.

The dinuclear complexes **7**, **9**, and **10** have slightly longer Pt–S bonds, as expected from the bridging nature of the formally monoanionic thiolate. Interestingly, the two Pt–S bonds in **7** and **9** are of different lengths, as are their respective Pt–C_{ax} bonds with, in each case, the segment with the shorter Pt–S bond showing a longer Pt–C_{ax} and vice versa, which is assigned to the *trans* influence. Complex **17** (PtMe₃Bphen-SC₆H₄CO₂Me) displays the longest Pt–S bond along with the shortest Pt–C_{ax} bond, resulting from the electron withdrawing –CO₂Me group reducing both the donor strength and *trans* influence of the thiolate.

Mechanistic Studies of Dinuclear Complex Formation and Oxidation. In addition to the above observations of the formation of dinuclear complexes and sulfates, further

Scheme 3. $2 \text{ PtMe}_3\text{dppzSC}_6\text{H}_4\text{-4-CO}_2\text{Me} \rightleftharpoons [(\text{PtMe}_3\text{dppz})_2\text{SC}_6\text{H}_4\text{-4-CO}_2\text{Me}]^+ 7$ Figure 1. Thermal ellipsoid plots of $\text{Me}_3\text{dppzPtSC}_6\text{H}_4\text{-4-CO}_2\text{Me}$ 6 (LHS) and the cationic fragment of $[(\text{Me}_3\text{dppzPt})_2\text{SC}_6\text{H}_4\text{-4-CO}_2\text{Me}]\text{PF}_6$ 7 (RHS) (hydrogen atoms omitted for clarity).Scheme 4. Synthesis of $\text{Me}_3\text{bpyPtSPh}$ 11Figure 2. Thermal ellipsoid plot of $\text{Me}_3\text{bpyPtSPh}$ 11 (hydrogen atoms omitted for clarity).Scheme 5. Synthesis of $\text{Me}_3\text{PhenPtSO}_2\text{-4-C}_6\text{H}_4\text{-CO}_2\text{Me}$ 12Figure 3. Thermal ellipsoid plot of $\text{Me}_3\text{PhenPtSO}_2\text{-4-C}_6\text{H}_4\text{-CO}_2\text{Me}$ 12 (hydrogen atoms omitted for clarity).

information regarding the degradation of these complexes came from the study of the degradation of $\text{PtMe}_3\text{BpySC}_6\text{H}_4\text{-CO}_2\text{Me}$, 22. 22 had previously been reported to be stable;¹⁴ however, a solution of 22 in CDCl_3 which had been aged for 6 weeks yielded two different types of crystals which X-ray diffraction revealed to be chlorotrimethyl-(2,2'-bipyridine)-platinum(IV), previously uncharacterized by crystallography, but closely related to the iodo- and bromo-analogues which have been,²⁹ and 4-mercaptomethylbenzoate disulfide.¹⁵ The abstraction of chloride from chloroform and displacement of the thiolate hinted at a more complex chemistry than simple aerobic oxidation of coordinated thiols to sulfinates and an equilibrium of mononuclear and dinuclear species which had been observed above.

In order to further investigate the degradation of 22, it was studied in CD_3CN in order to avoid halide exchange phenomena, deliberately exposing the sample to air over 72 h and following the changes by ^1H NMR. NMR analysis revealed that at least three products were present which DOSY

Table 1. Indications of Product Nature from Crystallographic and NMR Data^a

N^N	4-R-Ar-SH, R =	product type	number	crystal structure (counterion; origin)	NMR data
DPPZ	CO ₂ Me	mono⇌dinuclear	6	mononuclear	equilibrium 6–7
DPPZ	CO ₂ Me	dinuclear	7	dinuclear (PF ₆ [−] added)	
Bpy	OMe	mononuclear	8		equilibrium 8–9
Bpy	OMe	dinuclear	9	dinuclear complex (S ₂ O ₇ ^{2−} ; from MgSO ₄)	
Bpy	OMe	dinuclear	10	dinuclear complex (4-MeO-Ar-SO ₃ [−] ; oxidation)	
Phen	H	mononuclear	11		mononuclear
Phen	CO ₂ Me	sulfinate	12		mononuclear
Phen	H	mono⇌dinuclear	13	thiolate	mono⇌dinuclear
Phen	OMe	mono⇌dinuclear	14		mono⇌dinuclear
BPhen	H	mononuclear	15	sulfinate	mononuclear
BPhen	OMe	mono⇌dinuclear	16		mono⇌dinuclear
BPhen	CO ₂ Me	mono⇌dinuclear	17/18	thiolate	mono⇌dinuclear
OMeBpy	H	mono⇌dinuclear	19		mono⇌dinuclear
OMeBpy	OMe	mono⇌dinuclear	20		mono⇌dinuclear
OMeBpy	CO ₂ Me	mononuclear	21	thiolate	mononuclear
Bpy	NO ₂	sulfinate	26	sulfinate	sulfinate
Phen	NO ₂	sulfinate	27	sulfinate	sulfinate
BPhen	NO ₂	sulfinate	28	sulfinate	sulfinate
DPPZ	NO ₂	sulfinate	29	sulfinate	sulfinate
OMeBpy	NO ₂	mononuclear	30	mononuclear	mononuclear

^aSee SI Scheme S2 for chemical structures of all substances.Table 2. Pt–S and Pt–C_{axial} Bond Lengths Obtained from X-ray Crystallography

complex	N^N ligand	S-ligand	Pt–S (Å)	Pt–C _{ax} (Å)
6	DPPZ	S-C ₆ H ₄ -CO ₂ Me	2.479	2.073
7i	DPPZ	S-C ₆ H ₄ -CO ₂ Me	2.567	2.043
7ii	(dinuclear, PF ₆ [−])		2.504	2.050
9i	bpy	S-C ₆ H ₄ -OMe	2.482	2.071
9ii	(dinuclear, S ₂ O ₄ ^{2−})		2.505	2.062
10	bpy	S-C ₆ H ₄ -OMe	2.493	2.064
10	(dinuclear, MeO-C ₆ H ₄ -SO ₃ ^{2−})		2.483	2.069
11	bpy	S-Ph	2.460	2.079
12	phen	SO ₂ -C ₆ H ₄ -CO ₂ Me	2.391	2.074
15	bathophen	SO ₂ -Ph	2.392	2.092
17	bathophen	S-C ₆ H ₄ -CO ₂ Me	2.552	2.042
21	4,4′-diOMe-bpy	S-C ₆ H ₄ -CO ₂ Me	2.480	2.064
26	Bpy	SO ₂ -C ₆ H ₄ -NO ₂	2.404	2.086
27	Phen	SO ₂ -C ₆ H ₄ -NO ₂	2.434	2.083
28	BPhen	SO ₂ -C ₆ H ₄ -NO ₂	2.411	2.064
29	DPPZ	SO ₂ -C ₆ H ₄ -NO ₂	2.456	2.112
30	4,4′-diOMe-bpy	S-C ₆ H ₄ -NO ₂	2.502	2.082

suggested had significantly different masses. Although molecular mass calculations from diffusion DOSY data are inaccurate for systems containing atoms heavier than sulfur, and the calculation has not been optimized for this solvent, the order of masses was clear from the diffusion coefficients, and comparison with the mononuclear complex **12** (previously characterized), and iodide **1** (previously characterized, no thiolate peaks), allowed the dinuclear complex (new species showing both bpy and thiolate peaks in a 2:1 ratio) and other heavier species to be identified in the mixture (Figure 4, Scheme 6).

A series of NMR experiments following the degradation of **22** (Scheme 6) and *in situ* prepared **24** (Scheme 7, Figure 5) under aerobic and anaerobic atmospheres and in amber and clear tubes demonstrated that the conversion of mononuclear complexes to dinuclear complexes and/or sulfates required both light and air and revealed a solution species differing in

exact chemical shift from, but of similar mass to, the mononuclear complexes, assigned as the sulfates. Under anaerobic conditions, the samples were stable even under irradiation (300 lm white LED light source; see SI for output profile), and, in the absence of light, aerobic samples were also stable. Following the photo-degradation of **22** and **24** and by comparing signals to known materials, and DOSY estimations of mass, the identity of the species (thiolate, dinuclear complex, disulfide, sulfonic acid, and sulfate complex) and the sequence of generation were determined (see SI for details of the reasoning behind identification of peaks).

Although, in some cases (e.g., **21**), appreciable levels of dinuclear complex were only observed under photooxidation conditions, it should be noted that all these complexes appear to exist in equilibrium with the dinuclear complexes, with the equilibrium position dependent upon substituents. In addition to the observation above of dinuclear complexes in the DPPZ

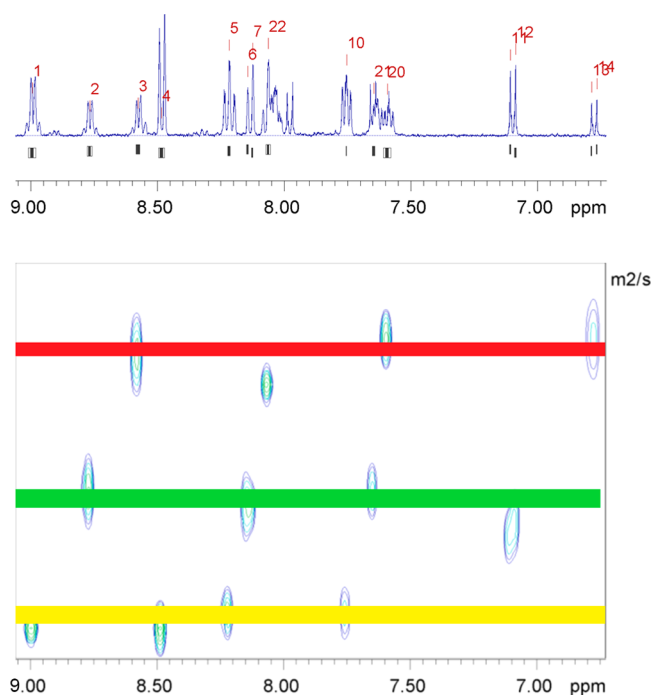


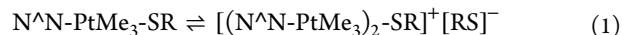
Figure 4. DOSY NMR showing the diffusion of dinuclear complex (red, $D_{AV} = 1.40 \times 10^{-9} \text{ m}^2/\text{s}$, mass = 959), mononuclear complex (green, $D_{AV} = 1.66 \times 10^{-9} \text{ m}^2/\text{s}$, mass = 563), and iodide 1 (yellow, $D_{AV} = 1.86 \times 10^{-9} \text{ m}^2/\text{s}$, mass = 523).

complex, 6, NMR experiments in degassed solutions in amber tubes using Bphen/4-MeOC₆H₄SH revealed that two major products, mononuclear and dinuclear, were present in a 3:1 ratio, whereas the Bpy/PhSH pair gives only the mononuclear complex even under aerobic conditions. Taken together, these findings suggest that the equilibrium position is ligand-dependent with more electron-rich thiols encouraging the formation of dinuclear complexes.

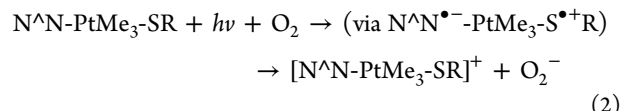
In summary, these platinum 1,2-diimine thiolate complexes appear to exist in equilibrium with thiol-bridged dinuclear complexes, with the equilibrium position being substituent-dependent; under irradiation and in the presence of air, the equilibrium shifts to favor dinuclear complexes as free thiol is converted to disulfides. The dinuclear complexes are then further S-oxidized to mononuclear sulfinate complexes, and upon prolonged irradiation, the sulfinate complexes are oxidized to the

sulfonic acids which dissociate. Meanwhile, the platinum complex reforms the starting iodide or an aqua complex.

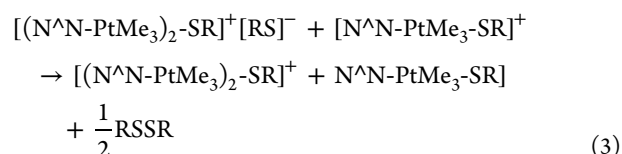
Summary of Steps. On the basis of these results, and the previous demonstration that the photo-excitation of these complexes involves charge transfer from the coordinated sulfur to the N[^]N ligand, a series of likely steps can be proposed (Scheme 8):



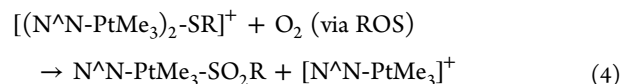
Mononuclear and dinuclear complex in equilibrium.



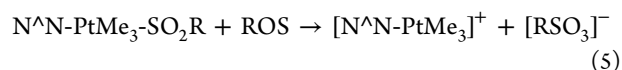
Photoexcitation to the excited state, followed by SET to O₂ (as both $h\nu$ and O₂ are required) with concomitant reduction of dioxygen to superoxide (other ROS cannot be excluded).



Oxidation of thiolate anion to disulfide by the radical cation derived from the photoexcited state of the mononuclear complex.



Oxidation of the bridging thiolate (stepwise or concerted) to the sulfinate complex with loss of the uncoordinated Pt core. We have no data concerning intermediates, but this step is only observed from the dinuclear complex.

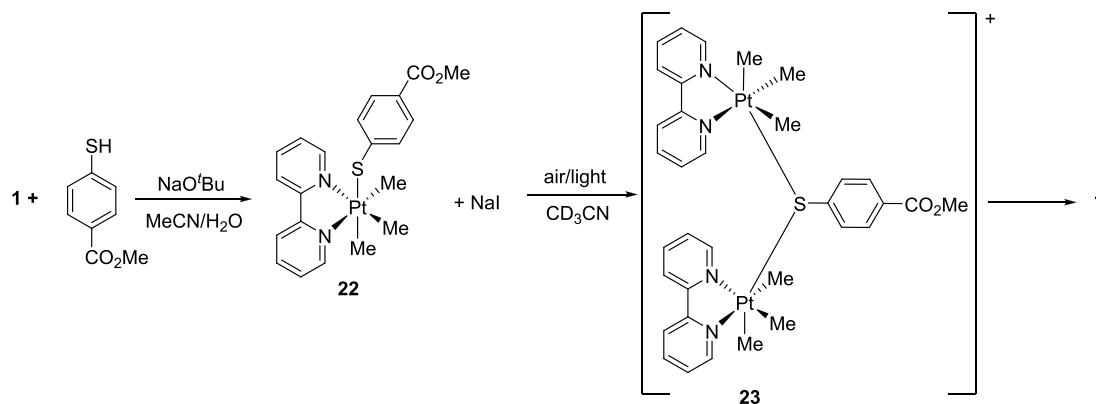


Oxidation of the sulfinate to the sulfonic acid.

The combination of steps 2 and 3 indicates that the complex photocatalyzes the oxidation of thiols to disulfides, which was supported by irradiating an NMR tube containing reduced glutathione and complex 22 in D₂O/d₃-MeCN which showed an irradiation-dependent oxidation to the disulfide form.

4-Nitrophenyl Sulfinate Complexes 26–29. The 4-nitrosulfinate complexes isolated from the reaction of 4-

Scheme 6. Decomposition of 22



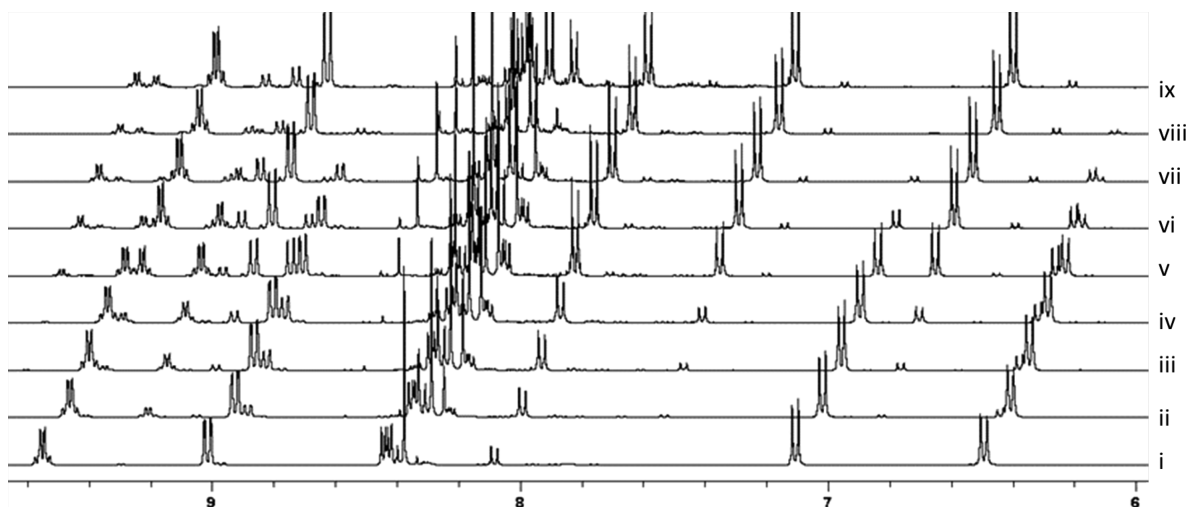
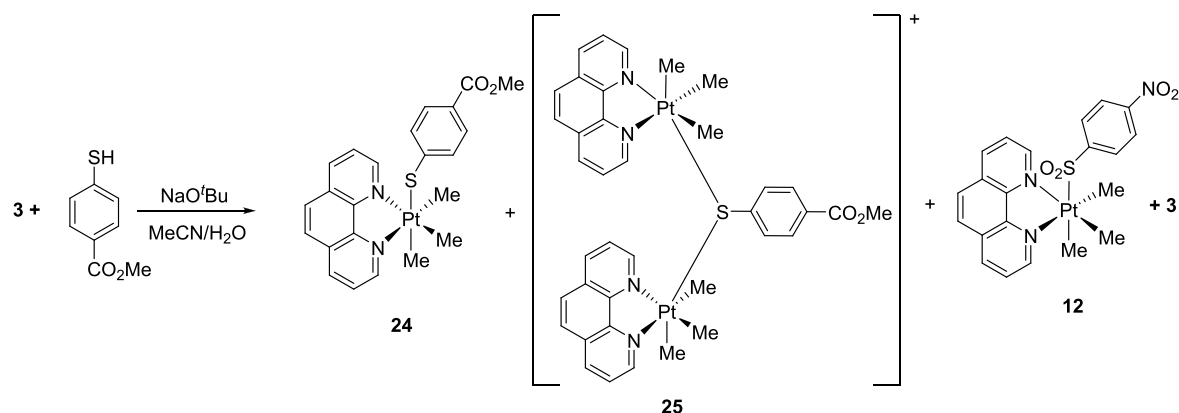
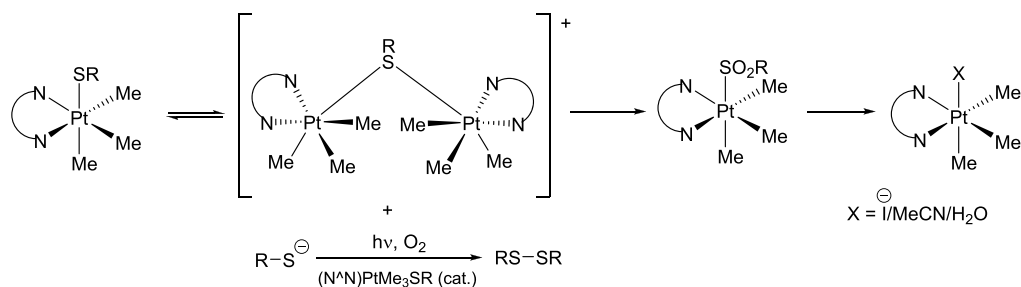
Scheme 7. Preparation and Photolytic Degradation of Me₃PhenPtS-4-C₆H₄-CO₂Me 24

Figure 5. NMRs of **24** (CD₃CN) over a period of exposure to air and light: (i) initial product; (ii) 30 min after exposure to air; (iii) irradiation for 1 h; (iv) irradiation for 3 h; (v) irradiation for 4 h; (vi) irradiation for 6.5 h; (vii) irradiation for 8.5 h; (viii) irradiation for 9.5 h; (ix) irradiation for 13.5 h in total.

Scheme 8. Suggested Pathway for the Decomposition of [(N^N)PtMe₃SR]

nitrothiophenol with complexes **1–4** were more stable than complexes previously discussed in this report, allowing partial characterization. Although these complexes are intrinsically unstable and degrade even in the solid state over several days, they were at least long-lived enough to allow NMR and photophysical characterization on clean materials. NMR analysis confirmed the mononuclear nature of the complexes, and IR spectra showed stretches tentatively assigned to S=O at higher wavenumber (average $\sim 1220\text{ cm}^{-1}$) than the Ni(II) precedents (average $\sim 1190\text{ cm}^{-1}$), in line with the higher oxidation state in the Pt(IV) complexes reducing the back-bonding and strengthening the S=O bonds. The reason for

the higher stability of sulfinate complexes derived from 4-nitrothiophenol compared to other thiols is not entirely clear, but may be related to Pt=S=O back-bonding. However, complex **30**, in which back-bonding to S=O should be maximized by the electron-donating 4,4'-dimethoxy-2,2'-bipyridine unit, was itself unstable and not able to be characterized beyond a crystal structure. The Pt–S bond lengths in the 4-nitrothiophenolate series (2.40–2.45 Å) are within the range of the two examples of sulfinate complexes previously discussed (2.39, 2.55 Å) which is compatible with, although not empirical evidence for, a back-bonding explanation. However, it should be noted that stability is a

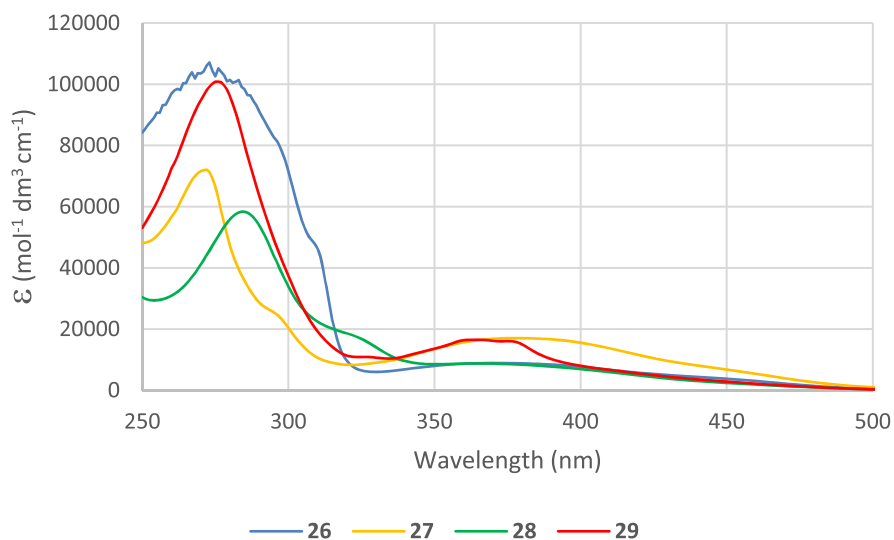


Figure 6. Absorption spectra of complexes 26–29 in MeCN.

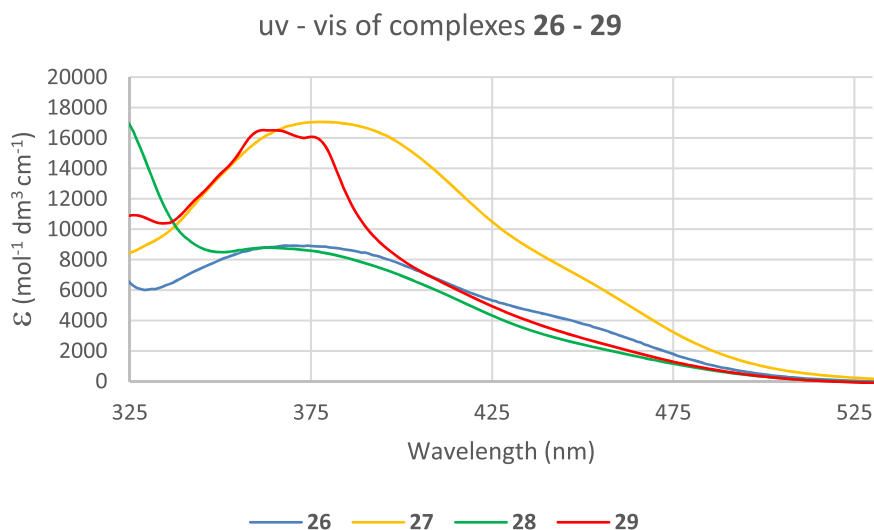


Figure 7. Expansion of absorption spectra of 26–29 between 325 and 530 nm.

Table 3. Excitation and Emission Data of Complexes 26–29 in MeCN

complex	1,2-diimine	$\lambda_{\text{max(abs)}} \text{ (nm); } \epsilon \text{ (mol}^{-1} \text{ dm}^3 \text{ cm}^{-1})$	$\lambda_{\text{max(ex)}} \text{ (nm)}$	$\lambda_{\text{max(em)}} \text{ (nm)}$	Θ_F^a	$\tau \text{ (ns)}$
26	2,2'-bipyridine	272(107094) 374(8612)	330	415	8.9×10^{-4}	1.24 ^b
27	1,10-phenanthroline	274(71323) 380(17046)	336	407	2.3×10^{-4}	N/A ^c
28	4,7-diphenyl-1,10-phenanthroline	291(57822) 366(8763)	342	456	9.7×10^{-4}	10.3 ^d
29	dipyrido[3,2-a:2',3'-c]phenazine	291(57822) 363(16499)	335	425	4.9×10^{-4}	N/A ^c

^aEstimated relative to standard;³⁰ see SI for details. ^bExcited at 405 nm, $\chi^2 = 1.024$. ^cNo excitation wavelength gave adequate counts. ^dExcited at 375 nm, $\chi^2 = 1.104$.

kinetic concept and bond length thermodynamic, and without much greater insight into the mechanism of loss of the sulfinate ligand, speculation about the bearing of back-bonding on the activation energy would be misguided.

Photophysical Characteristics of 4-Nitrophenyl Sulfinate Complexes 26–29. With a series of at least reasonably stable platinum(IV) trimethyl 1,2-diimine thiophenolate complexes finally available in the form of the oxidized sulfinate

series 26–29, their absorption and emission properties were studied in solution. Complexes 26–29 all display similar absorption spectra across a range of concentrations: they have a sharp, high energy peak between 273 and 286 nm (Figure 6) assigned to spin-allowed $\pi-\pi^*$ ligand transitions of the 1,2-diimines mixed with spin-allowed singlet MLCT ($d-\pi^*$) as previously reported for platinum trimethyl 1,2-diimines.^{13,14} In addition, there was a broad, lower energy peak of much lower

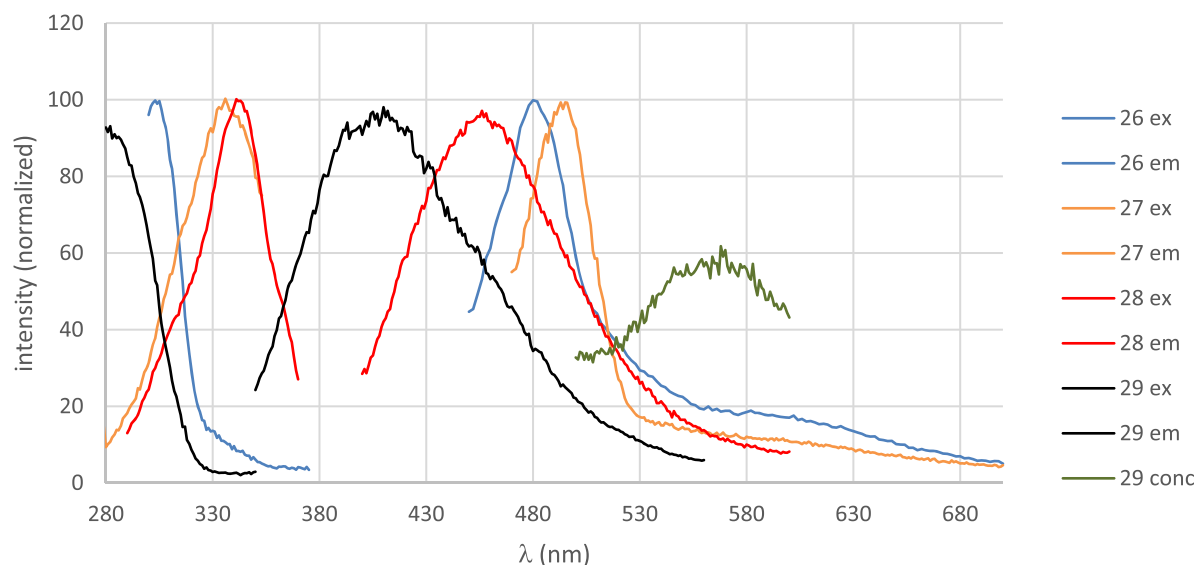


Figure 8. Excitation and emission spectra of complexes **26–29** in MeCN.

intensity between 364 and 485 nm (Figure 7) observed in all the complexes and which is the absorption band related to the characteristic colors of the complexes. The nature of this absorption band is discussed below.

In addition to the electronic absorption spectra, excitation and emission spectra were recorded of complexes **26–29** and revealed broad emission bands with maxima between 410 and 500 nm and broad excitation bands with maxima between 280 and 340 nm (see Table 3, Figure 8). They also show very weak broad shoulders tailing to low energy (>550 nm) which are only significant in weakly emitting, over-concentrated samples where they can appear stronger. This distortion is due to inner filter and absorption effects whereby, in the case of these complexes, the higher energy ends of the emission bands have significant overlap with the lower energy (non-emissive) absorption bands, biasing detection to the lower energy shoulders in concentrated samples. The luminescence quantum yields were determined to be between 0.02 and 0.1%, comparable to the previously reported values for PtMe₃(N^N)thiophenolates of 0.04%.¹⁴ TCSPC gave data which fitted well to single exponential decays solving to give luminescence lifetimes in the 1–10 ns region. The low energy shoulders are apparently of the same electronic origin as the main bands as no second lifetime component could be detected shifting the detection wavelength (although these data were poor due to weak counts). These excitation and emission characteristics are closely related to other reports of emission from platinum(IV) trimethyl 1,2-diimine complexes^{13,14} but are of interest as they appear to show that the low energy absorption detected in the UV–vis absorption spectrum leads to a non-emissive state, and that only excitation at higher energy populated an emissive state. The excitation spectra do not match the absorption spectra, with excitation maxima matching the low energy shoulder of the strongest absorption peaks centered around 300 nm, and with the low energy absorption bands in the visible region not reflected at all in the excitation spectra. It is expected that the lower energy shoulder of the strongest absorption bands reflects transitions in the more conjugated N^N ligands with higher energy contributions from the less conjugated aryl sulfinate unit, implying that the emissive state is localized on the conjugated

system. The lifetimes of 1–10 ns are short in comparison to triplet emitting transition-metal complexes, and as sensitivity to ³O₂ is a common probe for triplet states, lifetime measurements were recorded on degassed samples. There was very little change to the average lifetimes recorded (<1 ns), indicating that quenching by ³O₂ is not responsible for the fast decay of the excited states. As a comparison, the lifetime of Pt(Me₃)(bpy)-4-methoxycarbonylthiophenolate **22** which has previously been reported as a triplet emitter¹⁴ was recorded and found to be 5.6 ns. Finally, Pt(Me₃)(bpy)I, again a known triplet emitter,¹² was found to have a lifetime of 2.8 ns, indicating that these short lifetimes are typical of this core. In the light of these comparisons, the magnitude of the quantum yields, and the large Stokes shifts, it seems most likely that these complexes emit from triplet states but are quenched by structural features (e.g., the nine C–H bonds close to the location of the excited state) rather than ³O₂.

The orbital origin of the low energy absorbances was unclear, as the low energy absorbance bands responsible for visible light excitation of platinum(IV) trimethyl 1,2-diimine thiolates have been assigned as originating from excitation of electrons in a mixed Pt–S σ bonding and sulfur lone pair nonbonding electrons.¹⁴ As the sulfur in the sulfinate complexes has no nonbonding electrons, it seemed unlikely that the Pt–S σ orbitals could be the sole donor and further clarification was sought through theoretical work.

Theoretical Studies of Sulfinate Complexes. DFT calculations using the CAM-B3LYP level,³¹ with the 6-31+G(d,p) basis set on light atoms and SDD on Pt³² in simulated CH₃CN³³ indicated the HOMO of **26** to be a mixture of Pt–S and Pt–C_(Me-trans to S) σ -bonding orbitals and the LUMO of π^* character located on the 4-nitrothiophenolate ligand rather than the bipyridine (Figure 9). The LUMO+1 of **26** is also of π^* character but based on the bipyridine ligand, and approximately 0.47 eV higher in energy than the LUMO. HOMO–LUMO absorption is predicted to lie at 319 nm ($f = 0.058$), while HOMO–LUMO+1 is predicted to absorb at 292 nm ($f = 0.021$). The HOMO–1 orbital is of π character and based on the bipyridine ligand, giving a HOMO–1 to LUMO +1 (i.e., π to π^*) transition with strong absorption ($f = 0.33$) at 271 nm.

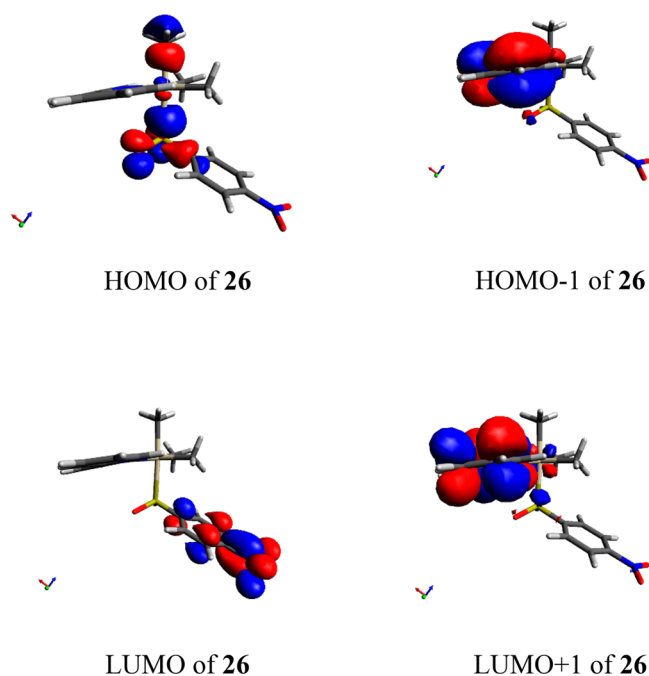


Figure 9. Molecular orbitals of complex 26.

In the light of these findings, we suggest that the lowest energy absorption observed in the spectra of **26–29** are assigned to a spin-allowed singlet HOMO→LUMO σ (Pt-S/Pt-C) $\rightarrow \pi^*$ (Ar-NO₂) transition, leading to a non-emissive excited state, while the higher energy excitations combine a HOMO→LUMO+1 σ (Pt-S/Pt-C) $\rightarrow \pi^*$ (1,2-diimine) transition, and a much stronger HOMO-1→LUMO+1 π to π^* transition, which leads to the emissive state, analogous to those observed in related complexes.^{12,14} It is unusual for a higher state not to relax into a lower one, but, given that relaxation into the Ar-NO₂-based state must be to the same spin multiplicity as the N[^]N state from which it originates, and given that the excitation to the Ar-NO₂-based singlet state is itself significantly lower energy than that to the N[^]N state, then assuming an Ar-NO₂-based triplet of even lower energy, intersystem crossing may be inefficient due to poor vibrational overlap of the states, in line with energy-gap law. For efficient relaxation between different sections of a luminophore without significant vibrational overlap, there is a requirement for a

dipole-dipole mechanism to allow relaxation of one state to populate the excited state of the other, and in the absence of this, it is common to see phenomena such as dual emission. In the case of complex **26**, the TD-DFT transition dipoles corresponding to absorptions at 319 and 292 nm are almost perpendicular ($\theta = 106.6^\circ$), possibly indicating an inefficient dipole-dipole coupling and therefore inefficient relaxation.

While the explanation for the lack of relaxation through the non-emissive LUMO (sulfinate-based) excited state is speculative, a novel excitation mechanism involving a σ (Pt-S/Pt-C) $\rightarrow \pi^*$ (Ar-NO₂) transition has been revealed by DFT methods. In addition to this unusual excited state, the emissive 1,2-diimine-based state has also been shown to be of an unusual origin, again involving a HOMO containing Pt–C σ bond character. To the best of our knowledge, transitions of these natures have not been previously reported.

In order to verify that the new transition discovered for complex **26** was a feature of the nitro-substituted thiophenol unit, analogous calculations were performed for the (unknown) nitro-free sulfinate complex PtMe₃(bpy)SO₂C₆H₅, **30**. The HOMO was again a mixture of Pt–S and Pt–C_(Me-trans to S) σ -bonding orbitals, but the LUMO in this case was the bipyridine π^* orbital, giving a HOMO→LUMO allowed singlet transition of similar character and energy to the HOMO→LUMO+1 transition of **29** (Figure 10). The HOMO-1 of **30** is of π^* character located on both the bipyridine and the thiolate, giving a HOMO-1→LUMO transition of $\pi \rightarrow \pi^*$ nature. Thus, while the low energy transition to the sulfinate π^* is unique to the nitro substituted case, it appears that the HOMOs of the sulfinate complexes are generally of Pt–S and Pt–C_(Me-trans to S) σ -bonding character. The existence of this relatively high energy HOMO in all oxidized complexes is significant in light of the observation that even oxidized complexes continue to show photooxidation ability; i.e., the loss of the thiolate lone pair does not preclude photocatalytic ability.

CONCLUSIONS

Although this study initially set out to explore the luminescent properties of platinum(IV) trimethyl bipyridyl thiolate complexes and their potential for luminescence applications, it is now apparent that there is a rich and complicated chemistry associated with these systems. These complexes appear to exist in dynamic equilibrium with dinuclear Pt(IV) S-bridged complexes, the position of the equilibrium being a

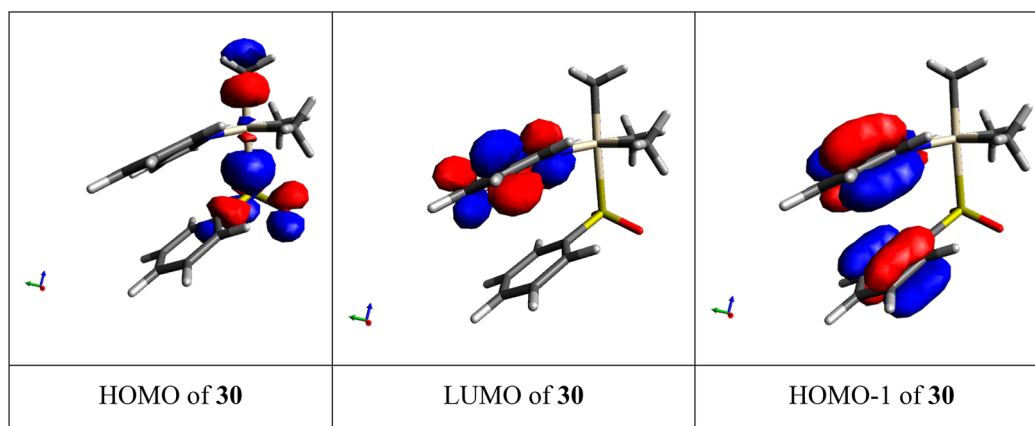


Figure 10. Molecular orbitals of **30**.

function of the nature of both the 1,2-diimine and thiolate ligands. The complexes show photochemical reactivity with visible light excitation with initial oxidation of the thiolate counterion trapping them in the dinuclear form, then photooxidation to the sulfinate complexes. There is precedent for dinuclear complex formation in Pt(Me₃)-1,2-diimine-based systems,²³ but there are no previous reports of Pt(IV) sulfinate. In a recent report, the closely related Re(CO)₃-1,2-diimine thiophenolates are described as undergoing degradation in solution to materials which have not been characterized but in which the NMR signals are similar to those observed in our photochemical oxidations.³⁴ Although a number of dinuclear and sulfinate complexes have been characterized by X-ray crystallography, and an outline mechanism for the transformation suggested by NMR studies, the sulfinate complexes are generally unstable and the sulfinate is displaced by solvent, water, or halides. However, sulfinate derived from 4-nitrothiophenol give complexes which are sufficiently stable to allow some degree of characterization to be undertaken. This stability can be rationalized in terms of back-bonding into the sulfinate π^* by the d⁶ Pt(IV) core. The sulfinate complexes show unusual photophysical behavior with excitations from a HOMO which is based in a mixed σ (Pt-S/Pt-C) bonding orbital to LUMOs of π^* symmetry based on either the N[^]N ligand, or, in the case of nitro-substituted species, the sulfinate aromatic ring. The transition to the sulfinate ring leads to a non-emissive state, while excitation to the N[^]N derived π^* orbitals gives emission with large Stokes shifts, and these states do not interconvert.

■ ASSOCIATED CONTENT

SI Supporting Information

The Supporting Information is available free of charge at <https://pubs.acs.org/doi/10.1021/acs.inorgchem.0c03553>.

Descriptions of experimental procedures and spectral data for the metastable complexes mentioned in the text; details of the analysis of NMR experiments pertinent to mechanistic work; decay and fitting data used to calculate the luminescence lifetimes; crystallographic data for all structures reported in the paper (PDF)

Accession Codes

CCDC 2013221–2013236, 2024113, 2025055, and 2025056 contain the supplementary crystallographic data for this paper. These data can be obtained free of charge via www.ccdc.cam.ac.uk/data_request/cif, or by emailing data_request@ccdc.cam.ac.uk, or by contacting The Cambridge Crystallographic Data Centre, 12 Union Road, Cambridge CB2 1EZ, UK; fax: +44 1223 336033.

■ AUTHOR INFORMATION

Corresponding Author

Michael P. Coogan – Department of Chemistry, University of Lancaster, Lancaster LA1 4YB, United Kingdom; orcid.org/0000-0003-2568-9337; Email: m.coogan@lancaster.ac.uk

Authors

Barbora Mala – Department of Chemistry, University of Lancaster, Lancaster LA1 4YB, United Kingdom

Laura E. Murtagh – Department of Chemistry, University of Lancaster, Lancaster LA1 4YB, United Kingdom

Charlotte M. A. Farrow – Department of Chemistry, University of Lancaster, Lancaster LA1 4YB, United Kingdom

Geoffrey R. Akien – Department of Chemistry, University of Lancaster, Lancaster LA1 4YB, United Kingdom

Nathan R. Halcovich – Department of Chemistry, University of Lancaster, Lancaster LA1 4YB, United Kingdom; orcid.org/0000-0001-6831-9681

Sarah L. Allinson – Department of Biomedical and Life Sciences, University of Lancaster, Lancaster LA1 4YG, United Kingdom

James A. Platts – School of Chemistry, Cardiff University, Cardiff CF10 3AT, United Kingdom; orcid.org/0000-0002-1008-6595

Complete contact information is available at:

<https://pubs.acs.org/doi/10.1021/acs.inorgchem.0c03553>

Author Contributions

^{||}These authors contributed equally. The manuscript was written through contributions of all authors. All authors have given approval to the final version of the manuscript.

Notes

The authors declare no competing financial interest.

■ ACKNOWLEDGMENTS

We thank Dr. David Rochester, Department of Chemistry, Lancaster University, for mass spectrometry and the Royal Society of Chemistry for a Royal Society of Chemistry Undergraduate Research Bursary (to C.M.A.F.).

■ REFERENCES

- (1) Ravelli, D.; Dondi, D.; Fagnoni, M.; Albini, A. Photocatalysis. A multi-faceted concept for green chemistry. *Chem. Soc. Rev.* **2009**, *38*, 1999–2011.
- (2) Chi, Y.; Chou, P.-T. Transition-metal phosphors with cyclo-metallating ligands: fundamentals and applications. *Chem. Soc. Rev.* **2010**, *39*, 638–655.
- (3) Nocera, D. G. Living healthy on a dying planet. *Chem. Soc. Rev.* **2009**, *38*, 13–15.
- (4) Fernandez-Moreira, V.; Thorp-Greenwood, F. L.; Coogan, M. P. Application of d6 transition metal complexes in fluorescence cell imaging. *Chem. Commun.* **2010**, *46*, 186–202.
- (5) Turner, E.; Bakken, N.; Li, J. Cyclometalated platinum complexes with luminescent quantum yields approaching 100%. *Inorg. Chem.* **2013**, *52* (13), 7344–7351.
- (6) Botchway, S. W.; Charnley, M.; Haycock, J. W.; Parker, A. W.; Rochester, D. L.; Weinstein, J. A.; Williams, J. A. G. Time-resolved and two-photon emission imaging microscopy of live cells with inert platinum complexes. *Proc. Natl. Acad. Sci. U. S. A.* **2008**, *105* (42), 16071–16076. Koo, C.-K.; Wong, K.; Man, W.-Y. C.; Lam, Y.-W.; So, K.-Y. L.; Tam, H.-L.; Tsao, S.-W.; Cheah, K.-W.; Lau, K.-C.; Yang, Y.-Y.; Chen, J.-C.; Lam, H.-W. M. A Bioaccumulative Cyclometalated Platinum(II) Complex with Two-Photon-Induced Emission for Live Cell Imaging. *Inorg. Chem.* **2009**, *48* (3), 872–878.
- (7) Juliá, F.; Bautista, D.; González-Herrero, P. Developing strongly luminescent platinum(IV) complexes: facile synthesis of bis-cyclometalated neutral emitters. *Chem. Commun.* **2016**, *52* (8), 1657–1660.
- (8) Chassot, L.; von Zelewsky, A.; Sandrini, D.; Maestri, M.; Balzani, V. Photochemical preparation of luminescent platinum(IV) complexes via oxidative addition on luminescent platinum(II) complexes. *J. Am. Chem. Soc.* **1986**, *108* (19), 6084–6085.
- (9) Abedi, A.; Amani, V.; Safari, N.; Ostad, S. N.; Notash, B. From proton transferred to cyclometalated platinum(IV) complex: Crystal

structure and biological activity. *J. Organomet. Chem.* **2015**, 799–800, 30–37.

(10) Juliá, F.; Bautista, D.; Fernández-Hernández, J. M.; González-Herrero, P. Homoleptic tris-cyclometalated platinum(IV) complexes: a new class of long-lived, highly efficient 3LC emitters. *Chem. Sci.* **2014**, 5, 1875.

(11) Pope, W. J.; Peachey, S. J. A new class of organo-metallic compounds. Preliminary notice. Trimethylplatinimethyl hydroxide and its salts. *Proc. Chem. Soc.* **1907**, 23, 86.

(12) Kunkely, H.; Vogler, A. Electronic spectra and photochemistry of methyl platinum(IV) complexes. *Coord. Chem. Rev.* **1991**, 111, 15–25. Hux, J. E.; Puddephatt, R. J. Photochemistry of mononuclear and binuclear tetramethylplatinum(IV) complexes: Reactivity of an organometallic free radical. *J. Organomet. Chem.* **1992**, 437 (1–2), 251–263. Hux, J. E.; Puddephatt, R. J. Photochemistry of tetramethyl(2,2'-bipyridine)platinum(IV). *J. Organomet. Chem.* **1988**, 346 (1), C31–C34. Mackay, F. S.; Farrer, N. J.; Salassa, L.; Tai, H.-C.; Deeth, R. J.; Moggach, S. A.; Wood, P. A.; Parsons, S.; Sadler, P. J. Synthesis, characterisation and photochemistry of Pt(IV) pyridyl azido acetato complexes. *Dalton Trans.* **2009**, 2315–2325.

(13) Hux, J. E.; Puddephatt, R. J. Reactivity of tetramethylplatinum(IV) complexes: Thermal reactions with electrophiles and unsaturated reagents. *Inorg. Chim. Acta* **1985**, 100 (1), 1–5. McCready, M. S.; Puddephatt, R. J. Oxidative addition of functional disulfides to platinum(II): Formation of chelating and bridging thiolate-carboxylate complexes of platinum(IV). *Inorg. Chem. Commun.* **2011**, 14, 210–212. Vetter, C.; Wagner, C.; Schmidt, J.; Steinborn, D. Synthesis and characterization of platinum(IV) complexes with N, S and S, S heterocyclic ligands. *Inorg. Chim. Acta* **2006**, 359 (13), 4326–4334. Brown, B.W.; Kite, K.; Nettle, A.J.; Psaila, A.F. Complexes of trimethylplatinum(IV) with dithiocarbamates, xanthates and cis-maleonitriledithiolate. *J. Organomet. Chem.* **1977**, 139 (1), C1–C3. Hall, J.R.; Swile, G.A. Proton NMR and infrared spectra of trimethylplatinum(IV) complexes of β -diketones. thio- β -diketones, and β -iminoketones. *J. Organomet. Chem.* **1973**, 47 (1), 195–215.

(14) Steel, H. L.; Allinson, S. L.; Andre, J.; Coogan, M. P.; Platts, J. A. Platinum trimethyl bipyridyl thiolates - New, tunable, red- to near IR emitting luminophores for bioimaging applications. *Chem. Commun.* **2015**, 51 (57), 11441–11444.

(15) Troyano, J.; Castillo, O.; Martinez, J. I.; Fernandez-Moreira, V.; Ballesteros, Y.; Maspoch, D.; Zamora, F.; Delgado, S. Reversible Thermochromic Polymeric Thin Films Made of Ultrathin 2D Crystals of Coordination Polymers Based on Copper(I) - Thiophenolates. *Adv. Funct. Mater.* **2018**, 28 (5), 1704040.

(16) Frisch, M. J.; Trucks, G. W.; Schlegel, H. B.; Scuseria, G. E.; Robb, M. A.; Cheeseman, J. R.; Scalmani, G.; Barone, V.; Mennucci, B.; Petersson, G. A.; Nakatsuji, H.; Caricato, M.; Li, X.; Hratchian, H. P.; Izmaylov, A. F.; Bloino, J.; Zheng, G.; Sonnenberg, J. L.; Hada, M.; Ehara, M.; Toyota, K.; Fukuda, R.; Hasegawa, J.; Ishida, M.; Nakajima, T.; Honda, Y.; Kitao, O.; Nakai, H.; Vreven, T.; Montgomery, J. A., Jr.; Peralta, J. E.; Ogliaro, F.; Bearpark, M.; Heyd, J. J.; Brothers, E.; Kudin, K. N.; Staroverov, V. N.; Keith, T.; Kobayashi, R.; Normand, J.; Raghavachari, K.; Rendell, A.; Burant, J. C.; Iyengar, S. S.; Tomasi, J.; Cossi, M.; Rega, N.; Millam, J. M.; Klene, M.; Knox, J. E.; Cross, J. B.; Bakken, V.; Adamo, C.; Jaramillo, J.; Gomperts, R.; Stratmann, R. E.; Yazyev, O.; Austin, A. J.; Cammi, R.; Pomelli, C.; Ochterski, J. W.; Martin, R. L.; Morokuma, K.; Zakrzewski, V. G.; Voth, G. A.; Salvador, P.; Dannenberg, J. J.; Dapprich, S.; Daniels, A. D.; Farkas, O.; Foresman, J. B.; Ortiz, J. V.; Cioslowski, J.; Fox, D. J. *Gaussian 09*, Rev. D.01; Gaussian, Inc.: Wallingford, CT, 2013.

(17) (a) Zhao, Y.; Truhlar, D. G. The M06 suite of density functionals for main group thermochemistry, thermochemical kinetics, noncovalent interactions, excited states, and transition elements: two new functionals and systematic testing of four M06-class functionals and 12 other functionals. *Theor. Chem. Acc.* **2008**, 120, 215–41. (b) Ditchfield, R.; Hehre, W. J.; Pople, J. A. Self-Consistent Molecular Orbital Methods. 9. Extended Gaussian-type basis for molecular-orbital studies of organic molecules. *J. Chem. Phys.*

1971, 54, 724. (c) Hariharan, P. C.; Pople, J. A. Influence of polarization functions on molecular-orbital hydrogenation energies. *Theor. Chem. Acc.* **1973**, 28, 213–22. (d) Andrae, D.; Hauessermann, U.; Dolg, M.; Stoll, H.; Preuss, H. Energy-adjusted ab initio pseudopotentials for the 2nd and 3rd row transition-elements. *Theor. Chem. Acc.* **1990**, 77, 123–41.

(18) Yanai, T.; Tew, D.; Handy, N. A new hybrid exchange-correlation functional using the Coulomb-attenuating method (CAM-B3LYP). *Chem. Phys. Lett.* **2004**, 393, 51–57.

(19) Tomasi, J.; Mennucci, B.; Cammi, R. Quantum mechanical continuum solvation models. *Chem. Rev.* **2005**, 105, 2999–3093.

(20) Dolomanov, O. V.; Bourhis, L. J.; Gildea, R. J.; Howard, J. A. K.; Puschmann, H. OLEX2: a complete structure solution, refinement and analysis program. *J. Appl. Crystallogr.* **2009**, 42, 339–341.

(21) Sheldrick, G. M. Crystal structure refinement with SHELXL. *Acta Crystallogr., Sect. C: Struct. Chem.* **2015**, C71, 3–8.

(22) Farrugia, L. J. WinGX and ORTEP for Windows: an update. *J. Appl. Crystallogr.* **2012**, 45, 849–854.

(23) Hill, G. S.; Vittal, J. J.; Puddephatt, R. J. Methyl(hydrido)-platinum(IV) Complexes: X-ray Structure of the First (μ -Hydrido)-diplatinum(IV) Complex. *Organometallics* **1997**, 16 (6), 1209–1217. Vance, B. Crystal structure of tetrakis(trimethyl- μ -S,S,N-thiocyanato-platinum), [$\text{Pt}(\text{CH}_3)_3\text{SCN}$]₄. *J. Organomet. Chem.* **1987**, 336 (3), 441. Ebert, K. H.; Massa, W.; Donath, H.; Lorberth, J.; Seo, B.-S.; Herdtweck, E. Organoplatinum compounds: VII. Trimethylplatinum thiomethylate and trimethylplatinum iodide. The crystal structures of [$(\text{CH}_3)_3\text{PtS}(\text{CH}_3)_4$] and [$(\text{CH}_3)_3\text{PtI}$]₄·0.5CH₃I. *J. Organomet. Chem.* **1998**, 559 (1–2), 203. Clegg, W.; Duran, N.; Fraser, K. A.; Gonzalez-Duarte, P.; Sola, J.; Taylor, I. C. New confacial bioctahedral diplatinum(IV) complexes with 3-aminoalkanthiolate bridges. *J. Chem. Soc., Dalton Trans.* **1993**, 23, 3453. Craig, D. C.; Dance, I. G. Molecular structure of tetrakis[benzenethiolatotrimethylplatinum(IV)], (μ_3 -SPH)₄(PtMe₃)₄. *Polyhedron* **1987**, 6 (5), 1157. Smith, G.; Kennard, C. H. L.; Mak, T. C. W. The crystal structure of tetrakis[trimethylthiomethyl-platinum(IV)], [$\text{Pt}(\text{CH}_3)_3(\text{SCH}_3)_4$]. *J. Organomet. Chem.* **1985**, 290 (1), c7–c10.

(24) (a) Morton, M. S.; Lachicotte, R. J.; Vicic, D. A.; Jones, W. D. Insertion of Elemental Sulfur and SO₂ into the Metal-Hydride and Metal-Carbon Bonds of Platinum Compounds. *Organometallics* **1999**, 18 (2), 227–234. (b) Hu, Y.; Wojcicki, A.; Calligaris, M.; Nardin, G. Reactions of coordinatively unsaturated platinum(II)-eta.1-allyl complexes with the electrophilic reagents sulfur dioxide, chlorosulfonyl isocyanate, and hexafluorophosphoric acid etherate. *Organometallics* **1987**, 6 (7), 1561. (c) Stace, J. J.; Ball, P. J.; Shingade, V.; Chatterjee, S.; Shiveley, A.; Fleeman, W. L.; Stanislawski, A. J.; Krause, J. A.; Connick, W. B. Kinetics of the methylation of a platinum(II) diimine dithiolate complex. *Inorg. Chim. Acta* **2016**, 447, 98. (d) Ishii, A.; Kashiura, S.; Hayashi, Y.; Weigand, W. Rearrangement of a (Dithiolato)platinum(II) Complex Formed by Reaction of Cyclic Disulfide 7,8-Dithiabicyclo[4.2.1]nona-2,4-diene with a Platinum(0) Complex: Oxidation of the Rearranged (Dithiolato)platinum(II) Complex. *Chem. - Eur. J.* **2007**, 13 (15), 4326. (e) Connick, W. B.; Gray, H. B. Photooxidation of Platinum(II) Diimine Dithiolates. *J. Am. Chem. Soc.* **1997**, 119 (48), 11620. (f) Hallock, J. S.; Galiano-Roth, A. S.; Collum, D. B. Organometallic chemistry of sulfonic acids. Highly stereo- and regioselective intramolecular hydroplatinations. X-ray crystal structure of (Ph₃P)₂Pt[trans-SO₂CH(CH₃)CH₂CH(CH₂CH₃)]. *Organometallics* **1988**, 7 (12), 2486. (g) Diamond, L. M.; Knight, F. R.; Cordes, D. B.; Fuller, A. L.; Slawin, A. M. Z.; Woollins, J. D. Platinum bisphosphine complexes of 1,8-naphthosultone. *Polyhedron* **2014**, 81, 356. (h) Oviedo, A.; Arevalo, A.; Flores-Alamo, M.; Garcia, J. J. Mechanistic Insights into the C-S Bond Breaking in Dibenzothiophene Sulfones. *Organometallics* **2012**, 31 (10), 4039. (i) Ishii, A.; Ohishi, M.; Nakata, N. Preparation of 3,3-Di-tert-butylthiirane trans-1,2-Dioxide and Its Reaction with a Platinum(0) Complex To Give a (Disulfenato)platinum(II) Complex: Regioselectivity of the Oxidation of a Related (Sulfenatothiolato)platinum(II) Complex. *Eur. J. Inorg. Chem.* **2007**, 2007 (33), 5199.

- (25) Aucott, S. M.; Milton, H. L.; Robertson, S. D.; Slawin, A. M. Z.; Walker, G. D.; Woollins, J. D. Platinum Complexes of Naphthalene-1,8-dichalcogen and Related Polyaromatic Hydrocarbon Ligands. *Chem. - Eur. J.* **2004**, *10* (7), 1666–1676.
- (26) Aucott, S. M.; Kilian, P.; Robertson, S. D.; Slawin, A. M. Z.; Woollins, J. D. Platinum Complexes of Dibenzo[1,2]Dithiin, Dibenzo[1,2]Dithiin Oxides and Related Polyaromatic Hydrocarbon Ligands. *Chem. - Eur. J.* **2006**, *12* (3), 895–902.
- (27) The Cambridge Crystallographic Data Centre (CCDC). <https://www.ccdc.cam.ac.uk/> (accessed 2021-02-4).
- (28) Buonomo, R. M.; Font, I.; Maguire, M. J.; Reibenspies, J. H.; Tuntulani, T.; Darensbourg, M. Y. Study of Sulfinate and Sulfenate Complexes Derived from the Oxygenation of Thiolate Sulfur in [1,5-Bis(2-mercapto-2-methylpropyl)-1,5-diazacyclooctanato(2-)]nickel(II). *J. Am. Chem. Soc.* **1995**, *117* (3), 963–973.
- (29) Nabavizadeh, S. M.; Habibzadeh, S.; Rashidi, M.; Puddephatt, R. J. Oxidative Addition of Ethyl Iodide to a Dimethylplatinum(II) Complex: Unusually Large Kinetic Isotope Effects and Their Transition-State Implications. *Organometallics* **2010**, *29* (23), 6359–6368.
- Momeni, B. Z.; Rashidi, M.; Jafari, M. M.; Patrick, B. O.; Abdel-Aziz, A. S. Oxidative addition of some mono, di or tetra haloalkanes to organoplatinum(II) complexes. *J. Organomet. Chem.* **2012**, *700*, 83–92.
- (30) Suzuki, K.; Kobayashi, A.; Kaneko, S.; Takehira, K.; Yoshihara, T.; Ishida, H.; Shiina, Y.; Oishi, S.; Tobita, S. Reevaluation of absolute luminescence quantum yields of standard solutions using a spectrometer with an integrating sphere and a back-thinned CCD detector. *Phys. Chem. Chem. Phys.* **2009**, *11*, 9850–9860.
- (31) Yanai, T.; Tew, D.; Handy, N. A new hybrid exchange-correlation functional using the Coulomb-attenuating method (CAM-B3LYP). *Chem. Phys. Lett.* **2004**, *393* (1–3), 51–57.
- (32) Ditchfield, R.; Hehre, W. J.; Pople, J. A. Self-Consistent Molecular-Orbital Methods. IX. An Extended Gaussian-Type Basis for Molecular-Orbital Studies of Organic Molecules. *J. Chem. Phys.* **1971**, *54*, 724.
- Hariharan, P. C.; Pople, J. A. The influence of polarization functions on molecular orbital hydrogenation energies. *Theor. Chem. Acc.* **1973**, *28*, 213–22.
- Andrae, D.; Haeussermann, U.; Dolg, M.; Stoll, H.; Preuss, H. Energy-adjusted ab initio pseudopotentials for the second and third row transition elements. *Theor. Chem. Acc.* **1990**, *77* (2), 123–41.
- (33) Tomasi, J.; Mennucci, B.; Cammi, R. Quantum Mechanical Continuum Solvation Models. *Chem. Rev.* **2005**, *105* (8), 2999–3093.
- (34) He, M.; Ching, H. Y. V.; Policar, C.; Bertrand, H. C. Rhenium tricarbonyl complexes with arenethiolate axial ligands. *New J. Chem.* **2018**, *42* (14), 11312–11323.